XIV Reunión de Trabajo Procesamiento de la Información y Control -- RPIC 2011, pp. 340-345, 2011.

A Voltage Sensorless Current Control for Inverters Connected to Distorted Grid Voltages

Sebastián Gómez Jorge† Jorge Solsona† Claudio Busada†

†*Instituto de Investigaciones en Ingeniería Eléctrica (IIIE) "Alfredo Desages" (UNS-CONICET).*
Departamento de Ingeniería Eléctrica y de Computadoras,
Universidad Nacional del Sur (UNS). (8000) Bahía Blanca, Argentina.
(e-mail: sebastian.gomezjorge@uns.edu.ar, jsolsona@uns.edu.ar, cbusada@uns.edu.ar)

***Abstract*— In this paper a sensorless current control for grid connected inverters is presented. The use of a grid voltage sensor is avoided, estimating the fundamental component and the harmonic content of the grid voltage via a reduced order observer. The proposed observer is frequency adaptive. The current control scheme is realized through a proportional resonant algorithm, using a scaled version of the estimated grid voltage fundamental component as current reference. The control algorithm is made frequency adaptive using the estimated frequency provided by the proposed observer. Simulation results are presented to validate the proposed scheme.**

***Keywords*— Distributed Generation, Sensorless Grid Current Control, Frequency Adaptive Control.**

1. Introduction

Nowadays the trend for the expansion of electric energy generation is the usage of distributed generation systems ([1], [15], [4], [3]). Most of these systems interact with the electric grid through the use of DC-AC converters ([5], [6]). To improve the reliability and reduce the cost it is desirable to use the minimum number of sensors. One option is to avoid the use of line voltage sensor, replacing it with an observer, which should estimate the grid voltage fundamental component and its harmonic content. There are several techniques for the estimation of sinusoidal signals ([16], [7]). In [10] a convergent variable frequency sinusoidal signal estimator is proposed for the case of a pure sinusoidal signal. In [9] a linear tracking-differentiator is proposed. The mathematic treatment given to the problem in this paper is simpler than the one in [10], still the estimation algorithm remains relatively complex, and it is only shown for the case of a pure sinusoidal signal. In [14] the results of [10] are extended to explicitly demonstrate the local convergence of the proposed algorithm in the presence of harmonics.

Besides the grid voltage estimation, an adequate control of the injected current it is necessary. In many distributed generation systems the main objective is to maximize the injected power and to minimize the harmonic distortion. One way to achieve this is to inject a sinusoidal current of fundamental frequency in phase with the fundamental component of the grid voltage. In [2] a deadbeat predictive current control is presented. The control scheme makes use of a grid voltage estimator based on the Adaptive Steepest Descent method and has power tracking steady state error compensation. Nevertheless, the results are shown for a pure sinusoidal grid with no harmonic content, and the proposed algorithm is not frequency adaptive. In [8] a sensorless resonant current control is proposed, where only the grid voltage is measured and a sliding mode observer is used to estimate the grid currents. There the results are also shown only for a pure sinusoidal grid with no harmonic content. In this case the proposed scheme is not frequency adaptive either. In [11] a grid voltage sensorless current controller for an unbalanced grid with harmonic content is presented. As in the previous articles, the proposed algorithm is not frequency adaptive.

In this paper a method to control the grid injected current which only requires the grid current and dc bus voltage measurements is proposed. This method allows to diminish the perturbation effect that the grid voltage imposes on the coupling inductance, enabling a simple current controller. It is also robust to grid frequency variations. The paper is organized as follows. In section 2 the proposed current control scheme is presented. In section 3 a pure sinusoidal grid voltage is considered. Afterwards, in section 4 a distorted grid voltage is considered. Finally, in section 5 simulation results are shown for both cases.

2. Control strategy with voltage sensor

In this section the current control scheme is presented. It is designed to track sinusoidal reference signals of fundamental grid voltage frequency with zero steady state error. Lets assume that the grid voltage v_g is known. If this is the case, then it is possible to try to cancel the perturbation effect of the grid voltage on the coupling inductance through a feedforward term

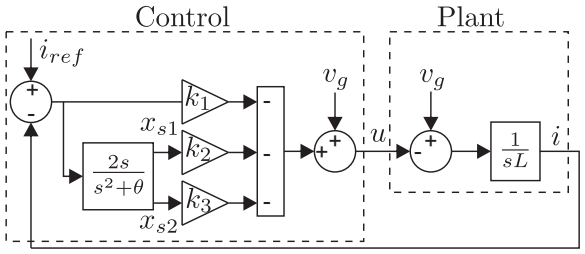

Figure 1: Controller.

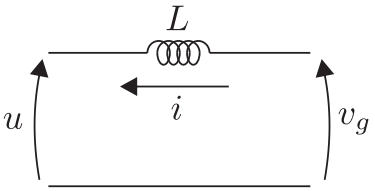

Figure 2: Grid coupling system model.

(see Fig. 1). This way the controller reduces to the current control on an inductance. To inject sinusoidal current in phase with the fundamental component of the grid voltage a second order generalized integrator (SOGI [18]) is implemented. When properly tuned, it yields zero steady state error to a sinusoidal reference current. In this case, the SOGI is tuned to the nominal grid frequency and a full state feedback is realized to ensure that the system is stable. The control scheme is shown in Fig. 1. In this figure the control action is $u = v_g - [k_1\ k_2\ k_3]\overrightarrow{X}$, where $\overrightarrow{X}$ is the system state vector. The feedback gains are computed in order to place the closed loop poles at the desired locations. To compute them, the system is described in the following state variable form:

$$\dot{\overrightarrow{X}} = A\overrightarrow{X} + Bu, \tag{1}$$

where $\overrightarrow{X} = [i\ x_{s1}\ x_{s2}]'$,

$$A = \begin{bmatrix} 0 & 0 & 0 \\ -2 & 0 & 1 \\ 0 & -\theta & 0 \end{bmatrix},\ B = \begin{bmatrix} -1/L \\ 0 \\ 0 \end{bmatrix},$$

where x_{s1} and x_{s2} are the SOGI states and $\theta = \omega^2$ is the square of the nominal steady state grid fundamental component angular frequency. The steady state closed loop poles are obtained finding the eigenvalues of $A - B[k_1\ k_2\ k_3]$. The gains can be chosen using the linear quadratic regulator method ([17]). The above proposed controller requires the use of a grid voltage sensor. In the following sections a grid voltage and fundamental frequency observer will be developed. The estimated voltage and frequency will be used to replace the measured voltage and to make the proposed controller frequency adaptive. This will be achieved by replacing v_g by $\hat{v}_g$ and θ by $\hat{\theta}$ in the block "Control" of Fig. 1. A comparison between the controller with measured and estimated grid voltage will be introduced in section 5 by means of simulation results.

3. Sensorless control in presence of a sinusoidal grid voltage

In this section the system model when the grid voltage is a pure sinusoid is presented. Based on this model an observer will be developed in order to estimate the grid voltage and frequency.

3. 1. System model

Figure 2 shows the coupling inductance that is usually used in distributed generation systems to interact with the grid (see plant block in Fig. 1). In this figure, u is the control voltage (which usually comes from an inverter), v_g is the grid voltage and i is the current. In this system the current is related to the voltage through,

$$\dot{i} = \frac{1}{L}(v_g - u). \tag{2}$$

Assuming that the grid voltage is a pure sinusoid given by $v_g = A\cos(\omega t + \phi)$, it is easy to see that v_g is solution to the following differential equation,

$$\ddot{v}_g + \theta\ v_g = 0,$$

where $\theta = \omega^2$. A possible representation of this equation in state variables is given by

$$\dot{x}_1 = \theta\ x_2,$$
$$\dot{x}_2 = -x_1,$$

where $v_g = x_1 = A\cos(\omega t + \phi)$ and $x_2 = -\frac{A}{\omega}\sin(\omega t + \phi)$. Then, using these equations and (2), and assuming θ constant, the system can be described by the following set of differential equations:

$$v_g = x_1, \tag{3}$$
$$\dot{i} = \frac{1}{L}(v_g - u), \tag{4}$$
$$\dot{x}_1 = \theta\ x_2, \tag{5}$$
$$\dot{x}_2 = -x_1, \tag{6}$$
$$\dot{\theta} = 0. \tag{7}$$

3. 2. Reduced order observer

A reduced order observer for the presented model will now be developed ([13], [12]). This observer allows to estimate the instantaneous value of the grid voltage and its fundamental component frequency.

From equations (5)-(7) the following observer is proposed,

$$\hat{v}_g = \hat{x}_1, \tag{8}$$
$$\dot{\hat{x}}_1 = \hat{\theta}\hat{x}_2 + g\ (v_g - \hat{v}_g), \tag{9}$$
$$\dot{\hat{x}}_2 = -\hat{x}_1, \tag{10}$$
$$\dot{\hat{\theta}} = al, \tag{11}$$

where g is an arbitrary positive constant which determines the convergence speed of the observer, and al is the adaptation law, that is defined to keep the system stable through Lyapunov's method. The observer as it is requieres the knowledge of the grid voltage v_g. To avoid the measurement of this signal, from (2) the following open loop model based estimator is proposed:

$$\dot{\hat{i}} = \frac{1}{L}(\hat{v}_g - u). \tag{12}$$

If this equation is subtracted to (2) then

$$v_g - \hat{v}_g = L(\dot{i} - \dot{\hat{i}}). \tag{13}$$

Replacing this equation in (9) and choosing the adaptation law al to keep the system stability, the proposed observer results,

$$\hat{v}_g = \hat{x}_1, \tag{14}$$
$$\dot{\hat{x}}_1 = \hat{\theta}\hat{x}_2 + g\ L(\dot{i} - \dot{\hat{i}}), \tag{15}$$
$$\dot{\hat{x}}_2 = -\hat{x}_1, \tag{16}$$
$$\dot{\hat{\theta}} = \gamma\ \hat{x}_2\ L(\dot{i} - \dot{\hat{i}}), \tag{17}$$

with γ an arbitrary positive constant that determines the convergence speed of the adaptation law. In the appendix the stability proof which leads to the obtention of al is shown.

As formulated in equations (14)-(17), the proposed observer needs the derivative of the current $\dot{i}$. To avoid computing this derivative a change of variables is proposed. First (12) is replaced in (15) and in (17) obtaining

$$\dot{\hat{x}}_1 = \hat{\theta}\hat{x}_2 + g\ L\dot{i} - g(\hat{v}_g - u), \tag{18}$$
$$\dot{\hat{\theta}} = \gamma\ \hat{x}_2\ L\dot{i} - \gamma\ \hat{x}_2(\hat{v}_g - u). \tag{19}$$

Then, the new variables are defined by subtracting the terms that contain $\dot{i}$ to the left hand side of these equations. That is,

$$\dot{\hat{v}}_1 = \dot{\hat{x}}_1 - g\ L\dot{i} = \hat{\theta}\hat{x}_2 - g(\hat{v}_g - u), \tag{20}$$
$$\dot{\hat{v}}_\theta = \dot{\hat{\theta}} - \gamma\ \hat{x}_2\ L\dot{i} = -\gamma\ \hat{x}_2(\hat{v}_g - u). \tag{21}$$

It is easy to see that $\hat{x}_1$ and $\hat{\theta}$ can be rewritten as a function of the new variables in the following way,

$$\hat{x}_1 = \hat{v}_1 + g\ Li, \tag{22}$$
$$\hat{\theta} = \hat{v}_\theta + \gamma\ L\int \hat{x}_2\ \dot{i}\ \delta t. \tag{23}$$

Equation (23) is solved by part integration, which leads to

$$\hat{\theta} = \hat{v}_\theta + \gamma\ L(\hat{x}_2\ i + \hat{v}_{aux}), \tag{24}$$
$$\dot{\hat{v}}_{aux} = -\dot{\hat{x}}_2\ i = \hat{x}_1\ i, \tag{25}$$

where the last equation was replaced with (16). Consequently, the resulting observer is described by the following set of differential equations:

$$\hat{x}_1 = \hat{v}_1 + g\ Li, \tag{26}$$
$$\hat{v}_g = \hat{x}_1, \tag{27}$$
$$\hat{\theta} = \hat{v}_\theta + \gamma\ L(\hat{x}_2\ i + \hat{v}_{aux}), \tag{28}$$
$$\dot{\hat{v}}_1 = \hat{\theta}\hat{x}_2 - g(\hat{v}_g - u), \tag{29}$$
$$\dot{\hat{x}}_2 = -\hat{x}_1, \tag{30}$$
$$\dot{\hat{v}}_\theta = -\gamma\ \hat{x}_2(\hat{v}_g - u), \tag{31}$$
$$\dot{\hat{v}}_{aux} = \hat{x}_1\ i, \tag{32}$$

As can be seen in these equations, the observer requires the measurement of only one output (the current i in the coupling inductance).

4. Sensorless control in presence of a distorted grid voltage

In this section the extended model to consider the case of a grid with harmonic content is presented. Based on this model an observer will be developed in order to estimate the grid voltage and frequency.

4. 1. Extended system model

Based on the model equations presented in section 3.1 and assuming that the grid only has an nth harmonic, the system is described by

$$v_g = x_1 + x_3, \tag{33}$$
$$\dot{i} = \frac{1}{L}(v_g - u), \tag{34}$$
$$\dot{x}_1 = \theta x_2, \tag{35}$$
$$\dot{x}_2 = -x_1, \tag{36}$$
$$\dot{x}_3 = n^2\theta x_4, \tag{37}$$
$$\dot{x}_4 = -x_3, \tag{38}$$
$$\dot{\theta} = 0, \tag{39}$$

where $x_1 = A\cos(\omega t + \phi)$, $x_2 = -\frac{A}{\omega}\sin(\omega t + \phi)$, $x_3 = A_n\cos(n\omega\ t + \phi_n)$, $x_4 = -\frac{A_n}{n\omega}\sin(n\omega\ t + \phi_n)$ and $\theta = \omega^2$.

4. 2. Extended Observer

Now the proposed observer will be extended to include an nth grid harmonic.

Based on the equations of the observer presented in section 3. 2 and the extended model presented in section 4. 1, the following observer is proposed for a

grid with an nth harmonic:

$$\hat{x}_1 = \hat{v}_1 + g_1\ L\ i, \tag{40}$$
$$\hat{x}_3 = \hat{v}_3 + g_2\ L\ i, \tag{41}$$
$$\hat{v}_g = \hat{x}_1 + \hat{x}_3, \tag{42}$$
$$\hat{\theta} = \hat{v}_\theta + \gamma L(\hat{x}_2\ i + \hat{v}_{aux}), \tag{43}$$
$$\dot{\hat{v}}_1 = \hat{\theta}\hat{x}_2 - g_1(\hat{v}_g - u), \tag{44}$$
$$\dot{\hat{x}}_2 = -\hat{x}_1, \tag{45}$$
$$\dot{\hat{v}}_3 = n^2\hat{\theta}\hat{x}_4 - g_2(\hat{v}_g - u), \tag{46}$$
$$\dot{\hat{x}}_4 = -\hat{x}_3, \tag{47}$$
$$\dot{\hat{v}}_\theta = -\gamma\hat{x}_2(\hat{v}_g - u), \tag{48}$$
$$\dot{\hat{v}}_{aux} = \hat{x}_1\ i, \tag{49}$$

where g_1 and g_2 are two arbitrary positive constants. $\hat{\theta}$ is saturated between $(2\pi 48)^2 < \hat{\theta} < (2\pi 52)^2$, since no global convergence proof is given at the time being. If the nth harmonic was a dc level then only one state would be required to estimate it. This state can be obtained making n in (46) equal to zero and eliminating equation (47).

Note that this observer can be used for the three-phase case if we consider that imbalances can be modeled through their positive and negative sequence components.

5. Simulation results

In this section simulation results are presented. A grid voltage with 5th, 7th, 11th and a DC level was used. Harmonic content rms values are shown in table 1. A coupling inductance $L = 1mHy$ is used in the simulations.

Table 1: Simulated grid harmonic content.

Harmonic N°	0°	1°	5°	7°	11°
Vrms	10	220	7.7	7.7	2.2

In figures 3, 4 and 6 simulation results for a grid with harmonic content are shown. In this case the grid has 5th, 7th, 11th harmonics plus a DC level. Figure 3a shows the reference current and the measured current for a controller with measured v_g. The reference current was $x_1/100$. The figure shows that the current almost instantly converges to the reference value. In Figure 3b the reference and measured currents are shown for the controller with estimated grid voltage and frequency. The reference current was set to be $\hat{x}_1/100$. As can be seen in this figure, the current quickly converges to the reference value, even though the frequency estimator has not converged yet (Figure 6). Figure 3c shows the error between the measured current and the reference current for the controller with measured v_g and estimated v_g. As shown, both cases have zero steady state error after the transient. In Figure 3d the grid voltage and estimated

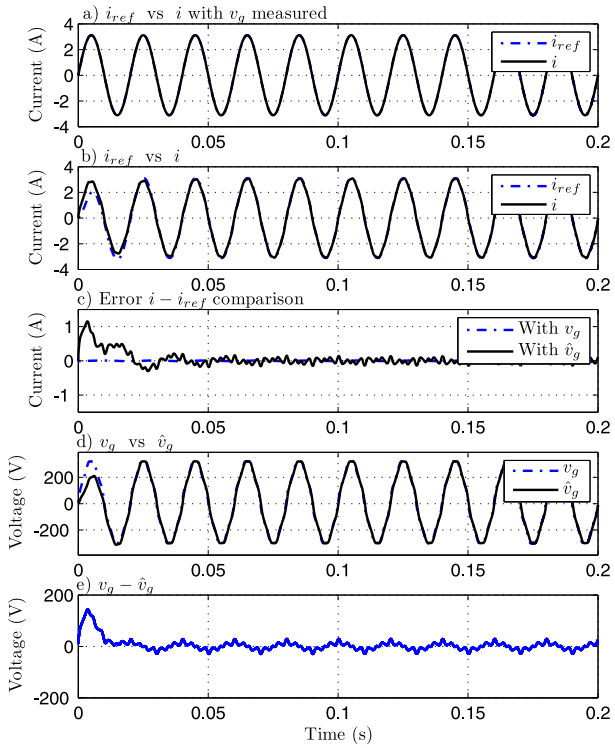

Figure 3: Grid with harmonic content. a) Reference current vs. measured current with measured v_g. b) Reference current vs. measured current with estimated v_g. c) Error between measured current and reference current for the controller with measured v_g and estimated v_g d) Grid voltage vs. estimated grid voltage. e) Error between the grid voltage and the estimated grid voltage.

grid voltage are shown. As can be seen in Figure 3e there is error between the actual and estimated values, since the frequency estimation has not converged yet. Figure 4 shows the same as Figure 3, but for the time instant where the frequency estimator converges to the grid fundamental component frequency. Figure 5 shows the fast Fourier transform (FFT) of the injected current. As can be seen, the total harmonic distortion (THD) is negligible. As shown in Figure 4c the grid voltage estimation error converges to zero. Finally, in Figure 6 the grid voltage fundamental component frequency and the estimated frequency are shown. A $0.5Hz$ frequency variation is introduced in order to appreciate the frequency tracking capabilities of the estimator. The simulation shows that the estimated frequency does not track the grid frequency during the transients with zero steady state error, but converges when the grid frequency reaches steady state. The convergence speed is slower than in the pure sinusoidal grid case. This is due to the saturation of the estimated frequency between 48Hz and 52Hz, since the estimator is not proven to be globally convergent.

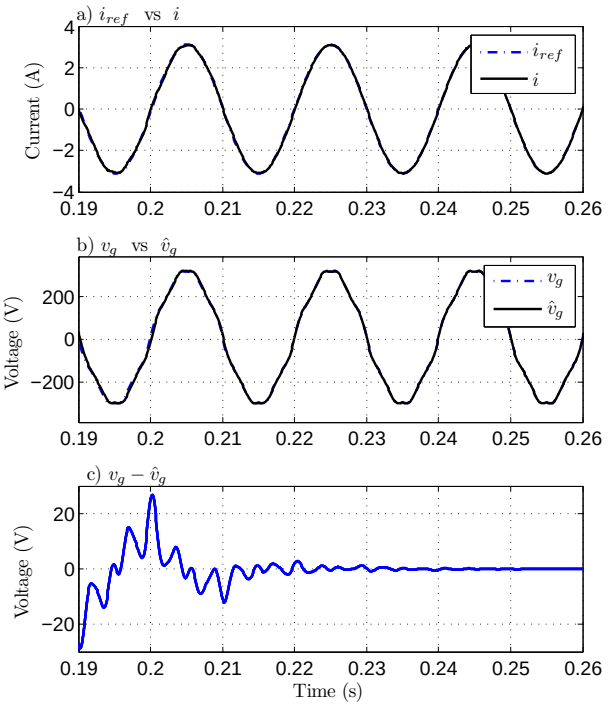

Figure 4: Grid with harmonic content. Zoom near $\hat{\theta}$ convergence time. a) Reference current vs. measured current. b) Grid voltage vs. estimated grid voltage. c) Error between the grid voltage and the estimated grid voltage.

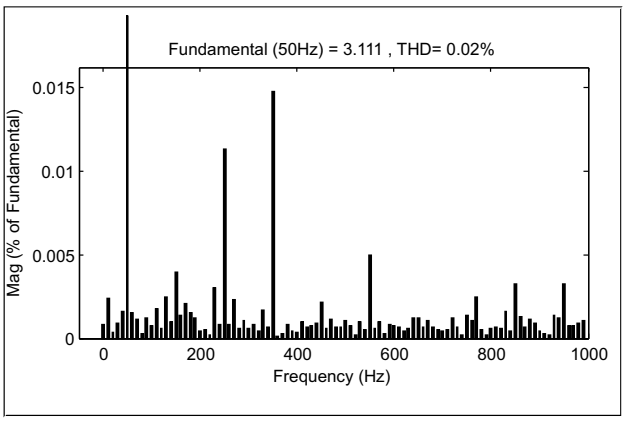

Figure 5: Grid with harmonic content. Injected current FFT.

6. Conclusions

A sensorless current control for distributed generation systems that avoids the use of grid voltage sensor has been presented. For a pure sinusoidal grid voltage a simple Lyapunov global convergence proof has been given, backed up by simulation results. The presented algorithm has also been shown to work empirically when the grid has harmonic content. Even though the results presented are for a single-phase case, the algorithm is easily extended for the three phase case.

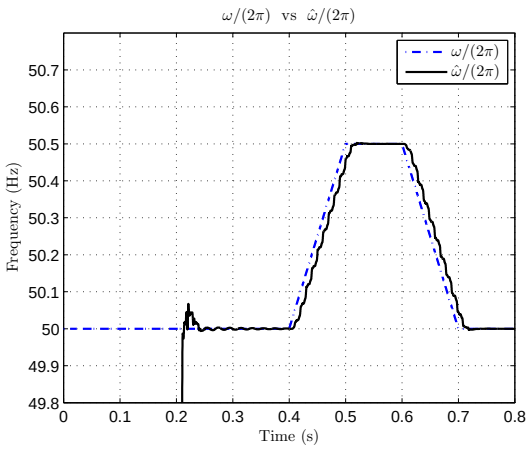

Figure 6: Grid with harmonic content. Grid frequency vs. estimated grid frequency.

7. Acknowledgments

This work was supported in part by Universidad Nacional del Sur under Grant PGI UNS 24/K045, Consejo Nacional de Investigaciones Científicas y Técnicas (CONICET) under Grant PIP CONICET 2671 and Agencia Nacional de Promoción Científica y Tecnológica (ANPCyT), Argentina.

Appendix

Let $e_{x1} = x_1 - \hat{x}_1$, $e_{x2} = x_2 - \hat{x}_2$ and $e_\theta = \theta - \hat{\theta}$ be the estimation errors. Then, subtracting (15) from (5) and (16) from (6), the derivatives of the error functions result:

$$\dot{e}_{x1} = \theta e_{x2} + e_\theta \hat{x}_2 - g e_{x1}, \tag{A1}$$

$$\dot{e}_{x2} = -e_{x1}, \tag{A2}$$

where (13) has been used to replace

$$L(\dot{i} - \dot{\hat{i}}) = e_{x1}.$$

Let

$$V = \frac{1}{2}\left(e_{x1}^2 + \theta e_{x2}^2 + \gamma^{-1} e_\theta^2\right)$$

be a candidate Lyapunov function, with γ an arbitrary positive constant, then, the derivative of the candidate function is given by,

$$\dot{V} = e_{x1}\dot{e}_{x1} + \theta e_{x2}\dot{e}_{x2} + \gamma^{-1} e_\theta \dot{e}_\theta.$$

Replacing (A1) and (A2) in this equation and operating, the following equation is obtained:

$$\dot{V} = -g e_{x1}^2 + \left(\hat{x}_2 e_{x1} + \gamma^{-1}\dot{e}_\theta\right)\ e_\theta.$$

In order for $\dot{V}$ to be negative it is necessary to make the second term of this equation equal zero, that is,

$$\hat{x}_2 e_{x1} + \gamma^{-1}\dot{e}_\theta = 0,$$

which implies that

$$\dot{\hat{\theta}} = \gamma\ \hat{x}_2 L(\dot{i} - \dot{\hat{i}}), \tag{A3}$$

that is the update algorithm for $\hat{\theta}$.

REFERENCES

[1] Editorial special issue on distributed power generation. *IEEE Transactions On Power Electronics*, 19(5):., September 2004.

[2] K.H. Ahmed, A.M. Massoud, S.J. Finney, and B.W. Williams. Stationary frame-based predictive sensorless current control with zero steady state error. *IEEE Power Electronics Specialists Conference*, pages 1495–1501, June 2008.

[3] A. Al-Salaymeh, Z. Al-Hamamre, F. Sharaf, and M.R. Abdelkader. Technical and economical assessment of the utilization of photovoltaic systems in residential buildings: The case of jordan. *Energy Conversion and Management*, 51(8):1719–1726, August 2011.

[4] L.M. Ayompe, S.J. Duffy, A. an McCormack, and M. Conlon. Measured performance of a 1.72 kw rooftop grid connected photovoltaic system in ireland. *Energy Conversion and Management*, 52(2):816–825, February 2011.

[5] Frede Blaabjerg, Zhe Chen, and Soeren Baekhoej. Power electronics as efficient interface in disperse power generation systems. *IEEE Transactions On Power Electronics*, 19(5):1184–1194, September 2004.

[6] Frede Blaabjerg, Remus Teodorescu, Marco Liserre, and Adrian V. Timbus. Overview of control and grid synchronization for distributed power generation systems. *Ieee Transactions On Industrial Electronics*, 53(5):1398–1409, October 2006.

[7] I. Djurovic. Estimation of the sinusoidal signal frequency based on the marginal median dft. *IEEE Transactions on Signal Processing*, 55(5):2043–2051, May 2007.

[8] S. Eren, M. Pahlevaninezhad, A. Bakhshai, and P. Jain. Grid-connected voltage source inverter for renewable energy conversion system with sensorless current control. *Twenty-Fifth Annual IEEE Applied Power Electronics Conference and Exposition*, pages 1048–2334, February 2010.

[9] Bao-Zhu Guot and Jing-Qing Han. A linear tracking-differentiator and application to the online estimation of the frequency of a sinusoidal signal. *Proceedings of the 2000 IEEE. International Conference on Control Applications*, September 2000.

[10] Liu Hsu, Romeo Ortega, and Gilney Damm. A globally convergent frequency estimator. *IEEE Transactions On Automatic Control*, 44(4):698–713, April 1999.

[11] K. Lee, T.M. Jahns, T.A. Lipo, V. Blasko, and R.D. Lorenz. Observer-based control methods for combined source-voltage harmonics and unbalance disturbances in pwm voltage-source converters. *IEEE Transactions on Industry Applications*, 45(6):2010–2021, September 2009.

[12] Andrés E. León and Jorge Alberto Solsona. Design of reduced-order nonlinear observers for energy conversion applications. *IET Control Theory and Applications*, 4(5):724–734, May 2010.

[13] Andrés E. León and Jorge Alberto Solsona. On state estimation in electric drives. *Energy Conversion and Management*, 51(3):600–605, March 2010.

[14] M. Mojiri and A. R. Bakhshai. An adaptive notch filter for frequency estimation of a periodic signal. *IEEE Transactions On Automatic Control*, 49(2):314–318, February 2004.

[15] Reza Nasiri and Ahmad Radan. Adaptive robust pole-placement control of 4-leg voltage-source inverters for standalone photovoltaic systems: Considering digital delays. *Energy Conversion and Management*, 52(2):1314–1324, February 2011.

[16] Y. Pantazis, O. Rosec, and Y. Stylianou. Iterative estimation of sinusoidal signal parameters. *IEEE Signal Processing Letters*, 17(5):461–464, May 2010.

[17] Charles L. Phillips and H. Troy Nagle. *Digital Control System Analysis and Design*. Prentice Hall, 1995.

[18] P. Rodriguez, A. Luna, I. Etxeberria, J.R. Hermoso, and R. Teodorescu. Multiple second order generalized integrators for harmonic synchronization of power converters. *IEEE Energy Conversion Congress and Exposition*, pages 2239–2246, September 2009.